Microchimica Acta
https://doi.org/10.1007/s00604-018-2861-z

ORIGINAL PAPER

Hyaluronic acid-grafted three-dimensional MWCNT array as biosensing interface for chronocoulometric detection and fluorometric imaging of CD44-overexpressing cancer cells

Minghuan Liu[1] · Yanan Xu[2] · Chusen Huang[2] · Ti Jia[2] · Xiaoyan Zhang[1] · Da-Peng Yang[1] · Nengqin Jia[2]

Received: 9 March 2018 / Accepted: 4 June 2018

Abstract

A sandwich-type electrochemical cytosensor is described for quantitative determination of CD44-overexpressing HeLa cells. Hyaluronic acid (HA) acts as a targeting molecule that was in-situ incorporated into the sensor based on the use of an indium tin oxide (ITO) electrode modified with multi-walled carbon nanotubes (MWCNTs). The 3D-MWCNT structure is shown to strongly improve the electronic properties and surface chemical reactivities. The HA-modified sensor exhibits a highly sensitive response to HeLa cells. A sandwiched hybridization protocol was then established using BIO [an N-butyl-4-(6′-aminohexyl) amino-1,8-naphthalimide probe modified with HA] as the tracing labels of the fluorescent probes for targeting CD44-positive tumor cells. The signal amplification was thereby maximized and measured by chronocoulometry. The binding of CD44-positive HeLa cells to the HA modified sensing layer causes a decrease in chronocoulometric response. The signal decreases linearly in the 2.1×10^2 to 2.1×10^7 HeLa cells·mL^{-1} concentration range with a detection limit of 70 cells·mL^{-1}. Such a sandwich-type assay may be tailored as a sensitive candidate for detecting low levels of tumor cells.

Keywords Non-enzymatic sensor · Fluorescence labeling · Chronocoulometry · HeLa cells · Hyaluronic acid

Introduction

Hyaluronic acid (HA), which is a biodegradable, biocompatible and non-immunogenic glycosaminoglycan, composed of repeating disaccharide units of D-glucuronic acid and (1-β-3)-N-acetyl-D-glucosamine. As a major component of the extracellular matrix, HA plays a vital role in a broad range of crucial biological and physiological processes, including cell growth, cell adhesion, cell-cell communication, signaling and organ structural stability [1–3]. HA with its binding proteins or receptors mediates a large number of biological events. For example, HA generates a key signal for activating the kinase pathways and regulating angiogenesis in tumors. The researches have been reported that CD44 is a transmembrane glycoprotein, which was the major receptor of HA in cancer cells and frequently employed HA as the drug carrier into the tumor with high CD44 expression [4]. Activated hyaluronate receptors (HR) are ubiquitously overexpressed by CD44 proteins for hyaluronan-mediated motility (RHAMM) on tumor cells [5, 6] that are lacking in their non-tumorigenic counterparts [7]. Therefore, CD44 receptor as a transmembrane glycoprotein (85 kDa) is essential for cellular functions, including migration, cell orientation, adhesion, and matrix-cell signaling processes [8]. Since the abnormal expression of CD44 proteins is observed in many solid tumor cells including lung breast, colorectal, renal, gastric, pancreatic, hepatocellular, and cervical cancer as well as melanoma [9–12], they can

Minghuan Liu and Yanan Xu contributed equally to this work.

Electronic supplementary material The online version of this article (https://doi.org/10.1007/s00604-018-2861-z) contains supplementary material, which is available to authorized users.

✉ Nengqin Jia
nqjia@shnu.edu.cn

Da-Peng Yang
yangdp@qztc.edu.cn

[1] College of Chemical Engineering and Materials Science, Quanzhou Normal University, Quanzhou 362000, Fujian Province, China

[2] The Education Ministry Key Laboratory of Resource Chemistry Shanghai Key Laboratory of Rare Earth Functional Materials and Shanghai Municipal Education Committee Key Laboratory of Molecular Imaging Probes and Sensors, Department of Chemistry, Shanghai Normal University, Shanghai 200234, China

Published online: 26 June 2018

act as a common marker for several cancer stem cells, which exhibit highly malignant and chemo-resistant properties [13]. Therefore, the high levels of CD44 proteins in cancer cells will become a potential biomarker for aggressive tumors in biological processes and clinical analysis. The conventional assay methods used for HA targeted imaging of tumor cells analysis mainly include magnetic resonance (MR) [14], HA-PEI system [15], and enzyme-linked immunosorbent assays (ELISA) [16], immuno-electrophoresis [17]. However, these methods normally need a time consuming labeling process, stringent laboratory conditions, and easy to fluorescence quenching. Thus, attempts to design and study a novel detecting method are valuable.

Chronocoulometry (CC) has been well known to be an effective approach to monitor the electrochemical determination of diffusion coefficients, electrode area, and adsorbed reactants [18–21]. A particular advantage of the method is that the charge for electrolysis of adsorbed species can be separated from double-layer charge of the electrode, enabling the use of chronocoulometry for characterizing the assembly process and determining surface concentrations on the electrode surface [18, 22, 23]. With its advantages of low cost, low background noise, high sensitivity, potential and spatial controllability, CC biosensor has been used in immunoassay, DNA analysis [24, 25], and interfacial properties monitoring [26, 27].

In this work, a sandwich-like cytosensor based on HA-MWCNT/ITO and a N-butyl-4-(6′-aminohexyl)amino-1,8-naphthalimide modified HA (BIO, which has exhibited highly selective for targeting CD44 overexpressed HeLa cells) [28] for fluorescence tracking of tumor cells was developed. The new fluorescent probe BIO (N-butyl-4-(6′-aminohexyl)amino-1,8-naphthalimide probe modified with HA) was synthesized (Scheme S1 in the Supporting Information) with a facile procedure. Herein, we selected naphthalimide as a fluorophore for synthesis of BIO probe. Compared to the other commercially available fluorescein (such as FAM), Rhodamine and cyanine dyes, naphthalimide has been demonstrated to be a photo-stable fluorophore. Especially under the continuous irradiation, there was no photobleaching observed in naphthalimide solution [28]. In addition, the convenient modification of the naphthalimide provides a mature synthetic procedure of BIO, which makes BIO easier to be obtained compared to the FAM modified HA. On the basis of the above advantages, BIO conforms to the high standard of an appropriate sensing probe for detecting and tracing research. The utilization of HA-MWCNT/ITO and BIO enhances the selectivity of this sandwich biosensor for sensing CD44 proteins on the cell surface. Besides, the assembled 3D-MWCNT structure on ITO electrode increases the surface area for immobilizing much HA and improve the electron transfer for enhancing electrochemical signals. When HA-based 3D-MWCNT modified ITO electrode bind to the cell surface, the high-expression of CD44 proteins of HeLa cells can be evaluated through the amplified CC signal of redox probe [Fe(CN)$_6$]$^{3-/4-}$. The HA-based biosensor can significantly respond to the change of cell quantity, and the corresponding fluorescent signal change is observed by fluorescence image and total fluorescence intensity (FI). Thus, these results prove the feasibility and reliability of analyzing tumor cells with CD44-positive expression via this HA-biosensor. This sensitive biosensor may provide an important tool to evaluate the CD44-overexpressing tumor cells and track the target directly by optical microscope technology with the fluorescent BIO synthesized target probes. Furthermore, this resultant HA@MWCNT based cytosensor exhibited a broad detection range with a fairly low detection limit of HeLa cells, offering a potential alternative method for tumor cell detection in clinical diagnosis with further efforts.

Experimental

Chemicals and materials

Indium tin oxide (ITO, resistivity = 10–15 Ω), MWCNT were obtained from Zhuhai Kaivo Co. and Shenzhen Nanotech Port Co, respectively. p-phenylenediamine (AP), Hyaluronic Acid were purchased from Aladdin. 1-(3-(dimethylamino)-propyl)-3-ethylcarbodiimide hydrochloride (EDC) and N-hydroxysuccinimide (NHS) were purchased from Sigma-Aldrich. Fetal bovine serum (FBS) and Dulbecco's Modified Eagle Medium (DMEM) were from Gibco. All other reagents were of analytical grade and were used as received. The ultrapure water (18.2 MΩ·cm) was used throughout the experiments.

Construction of 3D-MWCNT structure onto ITO surface

Indium tin oxide (ITO) electrodes (resistivity = 10–15 Ω) were ultrasonic washing in ultrahigh purity water (18.2 MΩ·cm), ethanol, acetone and isopropyl alcohol, separately. Then the electrochemical working area is controlled with a size of 2 mm × 3 mm via use of epoxy glue. For the preparation of arylamine film, in an ice bath, 10 mM p-phenylenediamine hydrochloric acid solution was rapidly added to 1 M $NaNO_2$ solution and allowed for 15 min complete reaction. The resultant diazonium cation was electrografted to the ITO by scanning once from 0.4 to −0.6 V vs SCE (v = 100 mV·s^{-1}), followed by depositing at −0.6 V for 2 min. Two final cyclic voltammetric scans were performed to confirm the passivation and hence grafting of the electrode.

Acid-treated functionalized MWCNT (5 mg, 1 mg·mL^{-1}) were dispersed in DMSO solution (5 mL) containing amide condensation agent HATU (5 mg, 1 mg·mL^{-1}), reacting for 30 min at room temperature. Then, the MWCNT were

vertically anchored to arylamine modified ITO electrodes at 65 °C for 24 h. After preparation, the 3D-MWCNT/ITO electrodes were rinsed with Phosphate buffered saline (PBS, 0.2 M, pH 7.4, containing 0.9% NaCl) and dried under a stream of nitrogen for the following modification.

Fabrication of the HA-MWCNT/ITO cytosensor

The ethylenediamine-modified HA (HA-NH_2) were firstly synthesized by linking the carboxyl groups on HA with the amino groups on ethylenediamine by EDC and NHS. In brief, HA (50 mg) was dissolved in pure water (15 mL), followed by the addition of 30-fold molar excess of ethylenediamine, EDC (135 mg) and NHS (135 mg). Then pH value of the solution was adjusted to 7.0 with 0.1 M HCl /NaOH and the mixture was stirred overnight. Finally, the HA-NH_2 were obtained by dialysis washing for 24 h, and freeze-drying. Following that, the previous 3D-MWCNT-ITO electrode was dipped into the HA-NH_2 solution, reacted for 3 h at 4 °C and washed with PBS (0.2 M, pH 7.4). After conjugation of HA-NH_2 with the activated carboxyl group of MWCNT via amide bond, the 3D-MWCNT@HA/ITO electrodes were obtained. The resulting electrodes were stored at 4 °C before use.

Synthesis of BIO fluorescent probe

BIO was synthesized according to the reported procedures. N-butyl-4-(6′-aminohexyl)amino-1,8-naphthalimide (BIO_2) was dissolved in DMSO. Sodium hyaluronate was dissolved in phosphate buffer (pH = 7.4) in an ice bath in another bottomed flask. After the HA was dissolved completely, EDC and NHS were added for the conjugation reaction between BIO_2 and HA. Concentrated HCl was added to adjust the pH of the resulting solution to 6.8, and then keeping activating for about 30 mins. Finally, the two solutions were mixed and ice bath was removed. The mixture was continued to stirring at room temperature for 12 h. The crude product was obtained through dialyzing with ultrapure water to remove unreacted reagents until the dialyzed ultrapure water becomes colorless, and then the orange solid was obtained after drying at a low temperature.

Cell culture, collection and fluorescent labeling

Cells were provided from the cell bank of Chinese Academy of Sciences. For easy visualization, all kinds of cells were cultured in a humidified incubator at 37 °C containing 5% CO_2, grown in Dulbecco's Modified Eagle Medium (DMEM) supplemented with fetal bovine serum (FBS, 10%, Gibco) and 1‰ P/S (*v*/v = penicillin/streptomycin, Gibco), Cells were collected at 1200 rpm for 5 min. Then, cells were suspended in PBS (0.2 M, pH 7.4) containing 1 mg/mL BIO probes and incubated at 37 °C for 30 min. Subsequently, the cell suspensions were centrifuged and washed with PBS three times until the supernatants were colorless. Thus, targeted fluorescently labeling BIO-cells were obtained. The prepared 3D-MWCNT@HA-ITO electrodes were then incubated in homogeneous cell-BIO suspensions at 37 °C for 2.5 h. After thoroughly rinsing with PBS, the cytosensors were used for fluorescent microscopy (OLYMPUS IX71) observations and electrochemical analysis.

Apparatus

Chronocoulometry, differential pulse voltammetry (DPV) and other electrochemical experiments were performed on a CHI 660B electrochemical workstation (Shanghai Chenhua Co. Ltd., China). A conventional three-electrode system was consisted of the functionalized ITO electrode as working electrode with SCE reference electrode and Pt wire counter electrode. The electrolyte solution included 10 mM $K_3Fe(CN)_6$/$K_4Fe(CN)_6$ (1:1) in a 10 mM PH 7.4 PBS. Chronocoulometry measurements were carried out with the following parameters: initial potential: −0.8 V; final potential: 0.5 V; number of steps: 2; pulse width: 0.25 s; pulse period: 250 ms. DPV measurements were performed from −0.2 to 0.6 V with a pulse amplitude of 50 mV and width of 0.02 s. Atomic force microscopy (AFM) images were acquired on at Multimode Nanoscope (Bruker AXS GmbH). Zeta potential was measured by Malvern Zetasizer Nano-zs 90.

Results and discussion

Ethylenediamine was covalently bound to the HA backbone using the conventional EDC chemistry. The surface modification of HA has been studied by zeta potential and FTIR analysis (Fig. 1). As shown in Fig. 1a, the zeta potential of ethylenediamine, HA and HA-ethylenediamine (HA-NH_2) is −4.94, −54.3 and − 16.8 mV, respectively. It can be seen that the surface potential of HA became positive after conjugation of ethylenediamine, which is attributed that at pH~7.0, the carboxyl groups of HA are ionized, and HA-NH_2 are positively charged. As indicated in Fig. 1b, pure HA exhibits a broad O-H stretching bond at ~3350 cm^{-1}, a shoulder peak at around 2900 cm^{-1} is associated with -CH_2, C = O stretching bond at 1300–1700 cm^{-1}. The typical bonds at 1660 cm^{-1} and 1655 cm^{-1} in HA-NH_2 conjugates are attributed to the CO-NH bond from HA. These apparent changes also indicated the successful surface modification of ethylenediamine onto HA.

In this study, the preparation of HA@MWCNT sensor film was a key step, in which 3D-MWCNT structure was built onto the surface of ITO electrode to accelerate the electron transfer rate and provide a favorable interface for the conjugation of HA-NH_2. AFM images on the 3D-MWCNT array modified

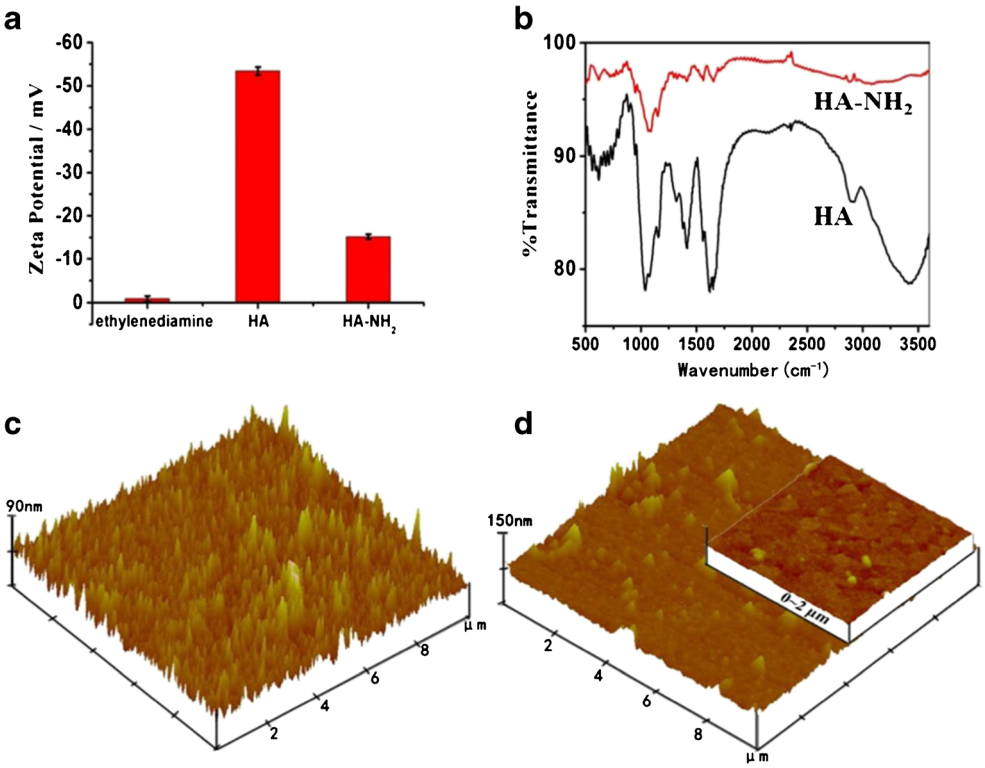

Fig. 1 **a** Zeta potential analysis of ethanediamine, HA and HA-NH2 in PBS solution. **b** FTIR spectra of HA and freeze dried HA-NH2 polymer. **c** AFM images of MWCNT modified ITO electrode and (**d**) MWCNT@HA modified ITO electrode

ITO electrode revealed an irregular, vertical assembly with a surface roughness of 6 ± 3 nm (Fig. 1c), while after HA-NH_2 molecules were covalently linked, the forest features of 3D-MWCNT array disappear and the surface roughness decreased to 4.55 ± 1 nm (Fig. 1d), suggesting that HA@MWCNT have been assembled on ITO electrode surface.

Further, Chronocoulometry and DPV measurements were carried out for the biosensor. Figure 2a shows CC diagrams were applied to confirm layer-by-layer assembling process of MWCNT-HA/ITO modified electrodes in the presence of $[Fe(CN)_6]^{3-/4-}$ as redox probe. At bare ITO electrode, the redox process of the probe shows a high CC intensity at 210 μC (curve a). After the electrochemical conjugation of arylamine on the electrode, CC intensity decrease to 65.3 μC (curve b), which is probably on account of the fact that generated arylamine layer can hinder the penetration of the redox probe. Upon the assembly of MWCNT array, the CC intensity increased to 113 μC, revealing a satisfactory electrical conductivity with the introduction of sensing matrix. After further modification of HA molecules, CC intensity obviously decreased to 55 μC (curve d) because of the poor conductivity of HA. After capture of HeLa cells (4.8×10^3 cells·mL^{-1}), the CC intensity greatly decreases (curve e) due to dielectric behavior of cells blocking the interfacial electron transfer process. Moreover, the successful assembly process of the HA-cytosensor can be also verified by DPV (Fig. 2b), which was consistent with the CC response.

As shown in Fig. 3a, DPV peak current at the cell captured cytosensor decreases gradually with the increasing incubating time, demonstrating more and more HeLa cells are being captured. A minimum DPV response obtained at 3 h expounds

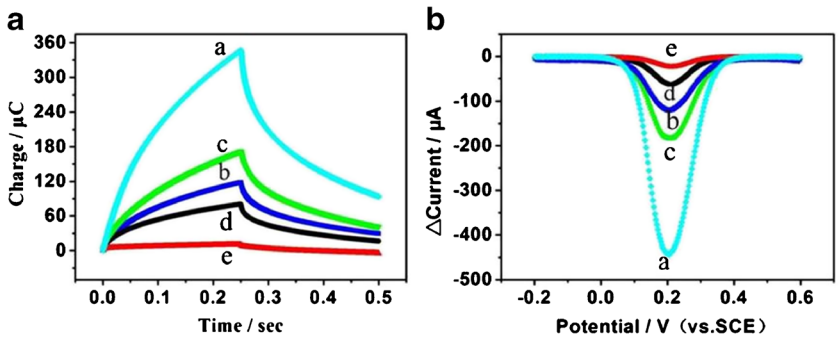

Fig. 2 **a** Chronocoulometric response of self-assemble process at different electrodes: (a) bare ITO, (b) arylamine modified ITO electrode, (c) MWCNT modified ITO electrode, HA@MWCNT modified ITO electrode before (d) and after (e) capture of BIO @ HeLa cells (4.8×10^3 cells·mL^{-1}). **b** The corresponding DPV response. The curve colors of DPV and CC are correspondent with each other

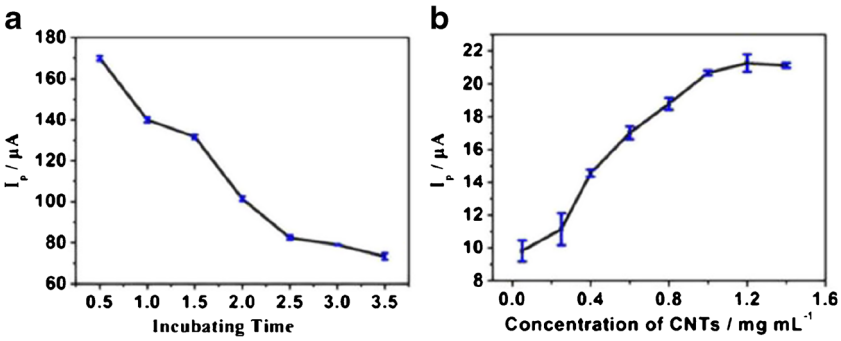

Fig. 3 DPV responses upon the biosensor at (**a**) different cellular incubating time and (**b**) different concentration of CNT (0.05, 0.25, 0.4, 0.6, 0.8, 1.0, 1.2, 1.4 mg·mL^{-1}) in the presence of 3.3×10^5 cells·mL^{-1} HeLa cells

that cells adhered to the modified electrodes has been saturated, showing enough sensitivity for HA- anchored detection of HeLa cells.

The concentration of CNT is an important parameter for amplifying electrochemical signals and sensitively detecting tumor cells. The DPV peak current presents a rising trend with the increasing concentration of CNTs, and then approaches to a maximum value at 1.0 mg·mL^{-1} (Fig. 3b). The DPV increment shows efficient surface area for HA loading and sufficient sensitivity for electrochemical biosensing of tumor cells.

Chronocoulometry has been utilized as a new alternative to develop electrochemical biosensors for detection of tumor cells. As to electrochemical reactions uncomplicated by chemical steps, the general mode of analyzing charge Q vs. t data was depicted using Anson plotting, assuming that plots of Q(t < T) vs. t1/2 and Qr = Q(T) – Q(t > T) vs. θ (θ = T1/2 + (t -T)1/2 -t1/2), are linear and both electrode double layer charging and adsorbed reactant electrolysis are instantaneous [18]. Thus, the chronocoulometric signals for each concentration can be generated using Anson plotting for the determination of specially captured tumor cells on the modified electrode. Herein, by using $[Fe(CN)_6]^{3-/4-}$ as the redox probe, CC measurements were applied to investigate the ability of target detecting tumor cells (e.g. HeLa cells). As comparison, we firstly investigated the HA-modified electrodes without 3D-MWCNT structure co-incubated with HeLa cells. It can be seen from Fig. S1A, when HeLa cells were adsorbed onto the HA film, the modified electrode showed an increased electron transfer resistance and thereby the decreasing of CC signal. Moreover, the charge value gradually decreased with the increasing of concentration of HeLa cells. The charge value (ΔQ) was proportional to the logarithm of HeLa cells concentration in the range of 1.5 × 103 to 6.2 × 106 cells·mL^{-1} (Fig. S1B). The linear equation can be depicted as ΔQ (μC) = −12.46 + 6.626 × lgC[HeLa] (cells·mL^{-1}) (R = 0.992). The detection limit of HA/ITO cytosensor is estimated to be approximately 5×10^2 cells·mL^{-1} (signal-to-noise, S/N = 3), indicating the HA/ITO electrode can be performed to quantitatively detect HeLa cells. However, upon the concentration of HeLa cells reduced to 1.5×10^3 cells·mL^{-1}, there is only slight variations in the Δ Charge which is shown in Fig. S1A.

To further improve its detection performances (eg. broad detection range and a low detection limit) of the cytosensor, MWCNT structure was attached onto the ITO electrode surface to construct a 3D sensing layer via the effect of strong amide linkage. This 3D-MWCNT structure can amplify the electrochemical current signal and provide sufficient loading area of HA molecules, leading to the greatly enhanced cell-capture affinity compared to the HA-ITO electrode. Figure 4a depicted the chronocoulometric responses of the cytosensor towards different cell concentrations, which were measured in the presence of $[Fe(CN)_6]^{3-/4-}$ as redox probe. With increasing concentration of labelled tumor cells, the charge value gradually decreased. The relationship between CC signal and logarithm concentrations of HeLa cells in the range from 2.1×10^2 to 2.1×10^7 cells·mL^{-1} was fitted linearly with the equation ΔQ (μC) = 29.90658 + 3.08247 × $lgC_{[HeLa]}$ (cells·mL^{-1}) with a correlation coefficient R = 0.996 (Fig. 4b). The detection limit (LOD) of the cytosensor is estimated to be approximately 70 cells·mL^{-1} (S/N = 3), which is much lower than those of 5×10^2 cells·mL^{-1} at the HA/ITO-based

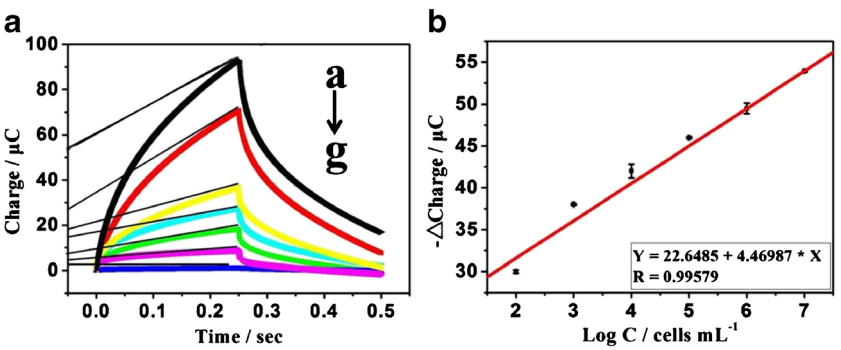

Fig. 4 **a** Typical chronocoulometric responses of the HA@MWCNT modified ITO electrode after adhesion with HeLa cells: (a) 0, (b) 2.1×10^2, (c) 2.1×10^3, (d) 2.1×10^4, (e) 2.1×10^5, (f) 2.1×10^6, (g) 2.1×10^7 cells·mL^{-1}. **b** A linear plot according to the CC signals for detecting HeLa cells

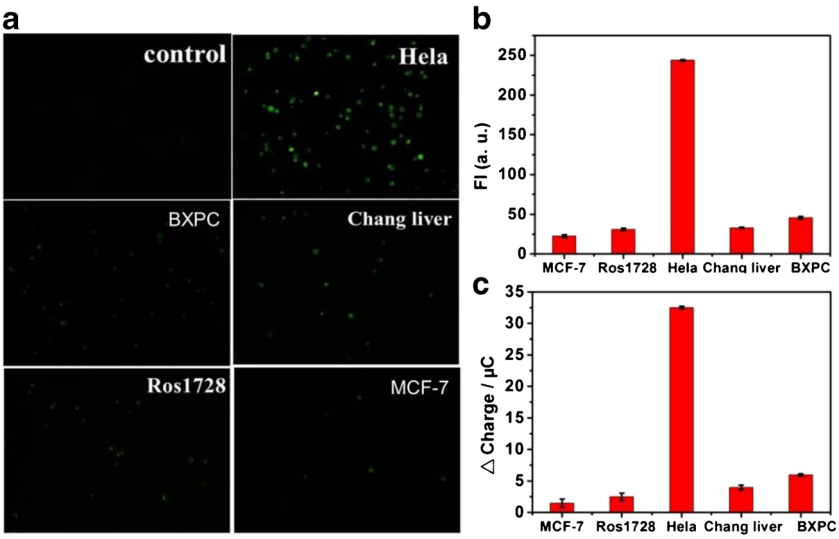

Fig. 5 **a** Changes in the fluorescence features of MCF-7 cells, ROS1728 cells, HeLa cells, Chang liver cells and BXPC-3 cells at the same concentration (1.3×104 cells·mL^{-1}) and a control system (HeLa cells without BIO probe). **b** The histogram is based on the total fluorescence intensity (FI) of each type of tumor cell in the displayed images. **c** Chronocoulometric responses of a BIO cytosensor upon HA@MWCNT modified ITO electrode toward various tumor cells

cytosensor, 2000 cells·mL^{-1} at an EIS sensor based on PANI-NF/AuNP electrochemical biosensor for HeLa cells [29], 250 HeLa cells·mL^{-1} at cyclic voltammetry sensor based on peptide nanotube–folic acid modified sensor [30], 300 HeLa cells·mL^{-1} at DPV sensor with Au/ITO using thioctic acid-based electrochemical immunoassay [31], and 90 cells mL^{-1} at EIS biosensor based on folate conjugated-PEI-CNT/GCE (Table S1 in the Supporting Information). Furthermore, the relative standard deviations (RSD) in the experimental intra-assay of the cytosensor were 4.2 and 5.1% at the cell concentrations of 2.1×10^5 and 2.1×10^6 cells·mL^{-1}, indicating its acceptable precision.

Notably, the detection range of chronocoulometric signal on the 3D-MWCNT@HA surface is much wider than that HA modified ITO planar surface, indicating a higher HA density on the former at the same area. Thus, the three-dimensional surface will provide a higher local ratio of cell affinitive HA to targeted cells than the planar surface in the following cell capture process. Furthermore, the 3D array can strengthen local topographic interactions between HA@MWCNT sensing layer and nanoscale elements of the cellular surface [32]. These morphologic differences between 3D-MWCNT@HA and HA modified ITO surfaces suggest that three-dimensional structure modified ITO biosensor may achieve more efficient capture by enhanced cell-substrate interactions. As our previously work reported [33], 3D-MWCNT structure has shown excellent performance in enhancement of surface area, superior electron transfer and efficient electrical conductivity.

In order to evaluate the specificity of the cytosensor, various types of cells including CD44 low expression cell lines MCF-7, BXPC-3, Chang liver, ROS 1728 and CD44 high expression HeLa cell lines were incubated with the cytosensor at the same cell concentration (1.0×10^4 cells·mL^{-1}), which were rapidly detected by both fluorescence microscopic technique and chronocoulometry. HeLa cells (1.0×10^4 cells·mL^{-1}) were also incubated on the fabricated cytosensor without BIO probe under the same experimental conditions as a control. As shown in Fig. 5a, the green fluorescence is significantly higher in HeLa cells with comparison to those of the other cells. The histogram based on the total fluorescence intensity (FI) of each cell line in the displayed images (Fig. 5b) also can clearly exhibit a high selectivity of the cytosensor for CD44-positive tumor cells. To confirm the specificity of the sandwich-like sensor, electrochemical analysis was further carried out using chronocoulometric methods under the same experimental conditions. The histogram of chronocoulometry signals are in good accordance with the fluorescence signals. It can be clearly observed from Fig. 5c that only HeLa cells result in an evident CC change with a chronocoulometric response of 32.5 μC, while CD44-low expression cells incubated at the cytosensor only cause five times less chronocoulometric signal of 5 μC, testifying this cytosensor is highly specific to CD44-positive tumor cells. Therefore, combined with the data presents in Fig. 5, it is concluded that this BIO cytosensor upon HA@MWCNT can be used to test and trace for the CD44+ and CD44-cells, even further to diagnose cancer with non-antibody-based biosensors.

Conclusions

In summary, this work describes a novel sandwich-like cytosensor. It is based on HA covalently anchored on 3D-MWCNT structure for ultrasensitive tumor cell determination via specific recognition of CD44 expression patterns on the cellular surface, and then BIO as the fluorescent probe to trace and dynamically evaluate the CD44-overexpressing tumor cells. Three-dimensional architecture MWCNT array performs stability, highly electrochemical activity. Furthermore,

the 3D-structure enhanced surface area can anchor much more amounts of HA in the cytosensor and enable for a highly selective and sensitive detection of overexpressed CD44 protein in cancer cells with a detection limit of 70 cells·mL^{-1}. These results illustrates that the chronocoulometry method has the advantages of higher sensitivity, lower background current, a broader detection range and a much lower detection limit. Besides, the study also reveals that BIO probe provides a dynamical tracking platform and a high specificity to CD44-positive tumor cells. With the combined advantages of bioconjugate techniques, fluorescence microscopy and CC detection, this strategy probably can be expanded to provide a feasible technique for early diagnosis of cancer in clinical application.

Acknowledgements This work was supported by the National Natural Science Foundation of China (81472001, 21373138 and 31400851), the Minjiang Scholars Program of Fujian Province, the Tongjiang Scholars Program of Quanzhou City and the Fourth Health Education Joint Development Project of Fujian Province (WKJ-2016-2-36).

Compliance with ethical standards The author(s) declare that they have no competing interests.

References

1. Yu M, Jambhrunkar S, Thorn P, Chen J, Gu W, Yu C (2013) Hyaluronic acid modified mesoporous silica nanoparticles for targeted drug delivery to CD44-overexpressing cancer cells. Nanoscale 5(1):178–183
2. Gui W, Zhang J, Chen X, Yu D, Ma Q (2018) N-doped graphene quantum dot@mesoporous silica nanoparticles modified with hyaluronic acid for fluorescent imaging of tumor cells and drug delivery. Microchim Acta 185:66
3. Wang W, Jayachandran S, Li M, Xu S, Luo X (2018) Hyaluronic acid functionalized nanostructured sensing interface for voltammetric determination of microRNA in biological media with ultra-high sensitivity and ultra-low fouling. Microchim Acta 185: 156
4. Gao N, Yang W, Nie H, Gong Y, Jing J, Gao L, Zhang X (2017) Turn-on theranostic fluorescent nanoprobe by electrostatic self-assembly of carbon dots with doxorubicin for targeted cancer cell imaging, in vivo hyaluronidase analysis, and targeted drug delivery. Biosens Bioelectron 96:300–307
5. Bourguignon LYW, Zhu H, Shao L, Chen YW (2000) CD44 interaction with tiam1 promotes Rac1 signaling and hyaluronic acid-mediated breast tumor cell migration. J Biol Chem 275:1829–1838
6. Platt VM, Szoka FC Jr (2008) Anticancer therapeutics: targeting macromolecules and nanocarriers to hyaluronan or CD44, a hyaluronan receptor. Mol Pharm 5(4):474–486
7. Datir SR, Das M, Singh RP, Jain S (2012) Hyaluronate tethered, "smart" multiwalled carbon nanotubes for tumor-targeted delivery of doxorubicin. Bioconjug Chem 23(11):2201–2213
8. Zhou B, Hao Y, Long D, Yang P (2018) Real-time quartz crystal microbalance cytosensor based on a signal recovery strategy for in-situ and continuous monitoring of multiple cell membrane glycoproteins. Biosens Bioelectron 111:90–96
9. Cho H-Y, Hossain MK, Lee J-H, Han J, Lee HJ, Kim K-J, Kim J-H, Lee K-B, Choi J-W (2018) Selective isolation and noninvasive analysis of circulating cancer stem cells through Raman imaging. Biosens Bioelectron 102:372–382
10. Coradini D, Zorzet S, Rossin R, Scarlata I, Pellizzaro C, Turrin C, Bello M, Cantoni S, Speranza A, Sava G, Mazzi U, Perbellini A (2004) Inhibition of hepatocellular carcinomas in vitro and hepatic metastases in vivo in mice by the histone deacetylase inhibitor HA-but. Clin Cancer Res 10(14):4822–4830
11. Choi KY, Min KH, Na JH, Choi K, Kim K, Park JH, Kwon IC, Jeong SY (2009) Self-assembled hyaluronic acid nanoparticles as a potential drug carrier for cancer therapy: synthesis, characterization, and in vivo biodistribution. J Mater Chem 19(24):4102–4107
12. Hyung W, Ko H, Park J, Lim E, Park SB, Park Y-J, Yoon HG, Suh JS, Haam S (2008) Novel hyaluronic acid (HA) coated drug carriers (HCDCs) for human breast cancer treatment. Biotechnol Bioeng 99 (2):442–454
13. Visvader JE, Lindeman GJ (2008) Cancer stem cells in solid tumours: accumulating evidence and unresolved questions. Nat Rev Cancer 8:755–768
14. Li J, He Y, Sun W, Luo Y, Cai H, Pan Y, Shen M, Xia J, Shi X (2014) Hyaluronic acid-modified hydrothermally synthesized iron oxide nanoparticles for targeted tumor MR imaging. Biomaterials 35(11):3666–3677
15. Tian H, Lin L, Chen J, Chen X, Park TG, Maruyama A (2011) RGD targeting hyaluronic acid coating system for PEI-PBLG polycation gene carriers. J Control Release 155(1):47–53
16. Li F, B-c B, Na K (2010) Acetylated hyaluronic acid/photosensitizer conjugate for the preparation of nanogels with controllable phototoxicity: synthesis, characterization, autophotoquenching properties, and in vitro phototoxicity against HeLa cells. Bioconjug Chem 21(7):1312–1320
17. Veillon P, Gallois Y, Moal V, Fouchard-Hubert I, Charles I, Larcher F, Dib N, Boursier J, Oberti F, Laafi J, Guechot J, Balan V, Cales P, Lunel-Fabiani F (2011) Assessment of new hyaluronic acid assays and their impact on FibroMeter scores. Clin Chim Acta 412(3–4): 347–352
18. Anson FC (1966) Innovations in the study of adsorbed reactants by chronocoulometry. Anal Chem 38(1):54–57
19. Zhong S-L, Zhuang J, Yang D-P, Tang D (2017) Eggshell membrane-templated synthesis of 3D hierarchical porous Au networks for electrochemical nonenzymatic glucose sensor. Biosens Bioelectron 96:26–32
20. Yang D-P, Guo W, Cai Z, Chen Y, He X, Huang C, Zhuang J, Jia N (2018) Highly sensitive electrochemiluminescence biosensor for cholesterol detection based on AgNPs-BSA-MnO_2 nanosheets with superior biocompatibility and synergistic catalytic activity. Sensors Actuators B Chem 260:642–649
21. Dana SM, Jablonski ME, Anderson MR (1993) Quantitative determination of surface excess by the semiintegral method. Anal Chem 65(8):1120–1122
22. Anjo DM, Corkery KK, Gonzalez E, Marantos KA, Estrada KE (1994) Diffusion coefficients of phenolic aromatics by chronocoulometry at the glassy-carbon electrode. J Chem Eng Data 39(4):813–816
23. Rusling JF, Brooks MY (1984) Analysis of chronocoulometric data and determination of surface concentrations. Anal Chem 56(12): 2147–2153
24. Ren R, Leng C, Zhang S (2010) Detection of DNA and indirect detection of tumor cells based on circular strand-replacement DNA polymerization on electrode. Chem Commun 46(31):5758–5760
25. Rasheed PA, Sandhyarani N (2017) Electrochemical DNA sensors based on the use of gold nanoparticles: a review on recent developments. Microchim Acta 184(4):981–1000
26. Dutta G, Kim S, Park S, Yang H (2014) Washing-free heterogeneous immunosensor using proximity-dependent electron mediation between an enzyme label and an electrode. Anal Chem 86(9): 4589–4595

27. Huang S, Feng M, Li J, Liu Y, Xiao Q (2018) Voltammetric determination of attomolar levels of a sequence derived from the genom of hepatitis B virus by using molecular beacon mediated circular strand displacement and rolling circle amplification. Microchim Acta 185:206
28. Jia T, Fu C, Huang C, Yang H, Jia N (2015) Highly sensitive naphth limide-based fluorescence polarization probe for detecting cancer cells. ACS Appl Mater Interfaces 7(18):10013–10021
29. Wang H, Wang T, Ye Y-X, Zhang Y-X, Yang P-H, Cai H-H, Cai J-Y (2012) Construction of an electrochemical cytosensor based on polyaniline nanofiber/gold nanoparticle interface and application to detection of cancer cells. Chin J Anal Chem 40(2):184–190
30. Castillo JJ, Svendsen WE, Rozlosnik N, Escobar P, Martinez F, Castillo-Leon J (2013) Detection of cancer cells using a peptide nanotube-folic acid modified graphene electrode. Analyst 138(4): 1026–1031
31. Wang X, Ju J, Li J, Li J, Qian Q, Mao C, Shen J (2014) Preparation of electrochemical cytosensor for sensitive detection of HeLa cells based on self-assembled monolayer. Electrochim Acta 123:511–517
32. Wang S, Wang H, Jiao J, Chen K-J, Owens GE, Kamei K-i, Sun J, Sherman DJ, Behrenbruch CP, Wu H, Tseng H-R (2009) Three-dimensional nanostructured substrates toward efficient capture of circulating tumor cells. Angew Chem 121(47):9132–9135
33. Xu Y, Wu H, Huang C, Hao C, Wu B, Miao C, Chen S, Jia N (2015) Sensitive detection of tumor cells by a new cytosensor with 3D-MWCNTs array based on vicinal-dithiol-containing proteins (VDPs). Biosens Bioelectron 66:321–326